



Science Arts & Métiers (SAM)

is an open access repository that collects the work of Arts et Métiers Institute of Technology researchers and makes it freely available over the web where possible.

This is an author-deposited version published in: <https://sam.ensam.eu>
Handle ID: <http://hdl.handle.net/10985/21763>

To cite this version :

Mohamed-Amine LARIBI, Sahbi TAMBOURA, Mohammadali SHIRINBAYAN, R. Tie BI, Hachmi BEN DALI, Abbas TCHARKHTCHI, Joseph FITOUSSI - Modeling of Short Fiber Reinforced Polymer Composites Subjected to Multiblock Loading - Applied Composite Materials - Vol. 28, n°4, p.973-990 - 2021

Any correspondence concerning this service should be sent to the repository

Administrator : scienceouverte@ensam.eu



Modeling of Short Fiber Reinforced Polymer Composites Subjected to Multi-block Loading

M. A. Laribi^{1,2} · S. Tamboura³ · J. Fitoussi² · M. Shirinbayan^{2,4} · R. Tie Bi⁵ · A. Tcharkhtchi² · H. Ben Dali³

Abstract

Short Fiber Reinforced Composite (SFRC) structures exhibit multiple microstructures (due to material flow during the process). They are generally subjected to variable amplitude loadings. In this context, a robust model is needed to predict fatigue life as a function of microstructure. In this paper, we propose a predictive micromechanical damage-based model allowing fatigue life prediction in the case of SFRC submitted to variable amplitude cyclic loading. An experimental study was firstly performed on Sheet Molding Compound (SMC) composite involving different microstructure configurations. Specimens were subjected to stress-controlled block loading. The influence of the order of the sequences was evaluated through Low-High amplitude (L-H) and High-Low amplitude (H-L) schemes. Damage accumulation is computed at the local scale to describe the evolution of the fiber-matrix interface damage until failure. A local failure criterion based on a critical damage state allowed predicting variable amplitude fatigue life as a function of microstructure. A good correlation was found between experimental and numerical results. Once the approach was validated, it has been used to model different useful variable amplitude loading schemes to emphasize the role of the loading sequence parameters and order.

Keywords Modeling · Micromechanical · Fatigue · Variable amplitude

1 Introduction

Fatigue characteristics under variable amplitude loadings differ from those obtained for constant amplitude one [1]. In the first case, crack propagation or crack evolution is significantly influenced by the history of the previous loading, which is known as the load sequence effect. In addition, a variable amplitude loading should imply a sudden variation that can accelerate the propagation of a discrete crack or increase the density of microcracks. In the case of heterogeneous materials such as composites, complex interactions between different damage mechanisms make a general law that allows predicting cumulative damage very difficult to establish. However, many of the existing damage

✉ M. A. Laribi
mohamed-Amine.Laribi@iut-tlse3.fr

accumulation based approaches proposed to model the variable amplitude fatigue response of composites have been based on theories developed for homogeneous metallic materials [2]. In fact, variable amplitude fatigue behavior of metallic materials including cumulative damage has been studied over the past decades [2, 3]. Damage quantification parameters and damage accumulation laws have been proposed. Indeed, in the literature, one can find several methods to characterize fatigue damage resulting from a variable amplitude loading [1–16]. The most recognized is the Palmgren-Miner's cumulative rule [4], where a linear damage increase is supposed until the critical state where $D=1$. In fact, failure generally happens for a critical value less than 1 according to the critical local state corresponding to the appearance of a critical crack. Therefore, one should use a critical rate D_c as the failure limit. This approach resulted in predictions with certain inaccuracies for sequential loadings. In addition, for composites, a loading sequence going from a low amplitude to a higher one has been reported as being more damaging than a loading sequence going from high to low amplitude while the opposite situation is generally observed for metallic materials [9]. Fatigue cumulative damage rules for continuous fiber composite polymers have been identified by Post et al. [2]. Miner's law has been reported to be non-conservative in most cases. In fact, models based on residual resistance, such as that proposed by Broutman and Sahu [5], have been proposed to give more precise predictions.

On the other hand, the behavior of polymeric materials such as (Short Fiber Reinforced Composite) SFRC under variable amplitude loadings has been much less studied. Indeed, complex interactions between different damage mechanisms, the influence of frequency, temperature and humidity on the fatigue behavior of polymer-based SFRC, make realistic damage accumulation laws and failure criterion difficult to establish.

Zago et al. [7] studied the cumulative fatigue damage of polyamide-based composites reinforced with short glass fibers in different orientations. Samples were tested under loading sequences at two amplitudes: low intensity (L-H) and high intensity (H-L). Based on the experimental results, a generalized non-linear Palmgren-Miner rule has been suggested to model the fatigue damage accumulation in the following form:

$$\sum \left(\frac{n_i}{N_i} \right)^b = 1$$

where n and N are the numbers of applied cycles at an applied stress σ_i and the corresponding number of cycles to failure, respectively. b is a material constant.

Zago and Springer [8], Sonsino and Moosbrugger [11] and Hartmann et al. [14] studied the fatigue behavior under variable amplitudes for certain composite materials with thermoplastic and thermosetting matrices. They also proposed damage accumulation based models to estimate the fatigue life. However, they require the use of many adjustment parameters from experimental data. These approaches are often inspired by the cumulative damage laws developed for metals. However, anisotropy and complex local damage mechanisms strongly affect SFRC fatigue failure, so that basic laws assumed to be isotropic and homogenous used for metals are not enough predictive.

In this paper, we used a new hybrid model [17] which combines phenomenological to micromechanical approach and allows predicting the fatigue life of SMC materials under a variable amplitude loading. Because the failure of SFRC is determined by local damage, the main idea of the developed approach is to consider that final failure always occurs when a critical amount of local damage, d_c , is reached. A micromechanical approach based on a Mori and Tanaka approach in which local damage is described by a local damage criterion is proposed. This damage model is used to establish an equation of state relating local damage rate

to macroscopic residual stiffness rate in the case of a monotonic loading. Damage accumulation is cumulated step by step and the evolution of the local damage rate, $\frac{d}{d_c}$, is identified. Failure happens when the local damage reach critical value “ d_c ”. The latter is identified by reverse engineering on the basis of the macroscopic tensile failure stresses of different microstructures. Because experimental evidence showed that the same damage and failure mechanisms are observed for monotonic and cyclic loading [18, 19], the equation of state describing the local damage rate evolution under monotonic loading is then generalized to fatigue loading. Therefore, the approach is adapted to multi-sequential thermomechanical loading based on the principle of superposition. Note that the proposed methodology integrates microstructure as input data so that it is a major asset of this predictive method.

In this paper, the methodology is presented. Then, it is applied in the case of variable loadings involving a succession of high and low blocks corresponding respectively to strong and low values of the applied stress. It is first applied in the case of two blocks of different amplitudes alternating until the rupture is obtained, (L-H) and (H-L). The method is validated by comparison with experimental results obtained on different types of microstructures (High Oriented material, HO and Randomly Oriented material, RO) in different directions of loading. An analysis of the reliability of the results is then proposed according to the types of sequences and microstructures.

Moreover, the effect of the sequence order is evaluated in the case of different two block schemes. Finally, once the model is validated through comparison between experimental and numerical results, it is applied in the cases of different multi-sequential thermomechanical loading schemes to emphasize several load sequence effects. Some practical conclusions are given to help structural design.

2 Material and Experimental Methods

2.1 Material

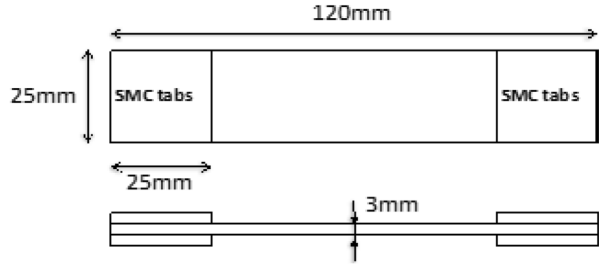
Sheet Molding Compound (SMC) composite is typically used in automotive exterior structures such as tailgates. SMC is a good mechanical performance material consisting of a polyester resin reinforced by glass fibers (28% in mass). Fibers are presented as chopped bundles of constant length ($L=25$ mm). Each bundle contains approximately 250 fibers of about $15\text{ }\mu\text{m}$ diameter. For this study, two types of microstructure presented in the form of plates have been provided by Faurecia Automotive, High Oriented (HO) plates and Randomly Oriented (RO) plates. HO plates have been obtained by placing the non-reticulate SMC only in half of the surface of a rectangular mold ($120\times 250\text{ mm}^2$) before thermo-compression. In that case, fibers tend to be oriented in the Mold Flow Direction. RO plates were provided by filling more than 80% of the mold surface in order to limit material flow. These plates are obtained under an average pressure of 60 Bars and a temperature of $165\text{ }^\circ\text{C}$.

2.2 Experimental Methods

2.2.1 Specimen Geometry

Figure 1 shows the used specimen geometry. The description of the specimen geometry was presented in the previous work [17]. This geometry was chosen to contain a representative elementary volume (REV) which takes into account the average length of the fibers.

Fig. 1 SMC specimen geometry



2.2.2 Test Configuration

Different mechanical tests have been performed using the MTS 830 servo-hydraulic testing machine with the capacity of 10kN:

- Quasi-static loading-unloading tensile tests have been performed at different increasing maximum stresses until failure. The determination of the Young's Modulus, E , during each reloading stage leads to the determination of the relative loss of stiffness, $\frac{E}{E_0}$, during monotonic loading.
- Tension-tension stress-controlled fatigue tests have been performed at different applied maximum stress (σ_{\max}). The minimum applied stress (σ_{\min}) is chosen to be equal to 10% of the maximum applied stress so the stress-ratio is $R=0.1$. The chosen frequency was $f=10$ Hz.
- In this paper, variable amplitude fatigue loading will be analyzed. Multi-stage block loadings at two amplitude levels (high-low (H-L) and low-high (H-L) applied alternatively) are illustrated in Fig. 2. The two loading blocks had the same ratio ($R=0.1$), each loading block contains the same number of cycles, followed by a cycle of higher amplitude. These two sequences are repeated until the break. H-L and L-H load sequences differ by the first sequence. H-L begins by the High amplitude block while L-H begins by the Low amplitude one.
- The second type of profile was simulated to highlight the parameters influencing the lifetime. This profile was studied by Fatemi et al. [1]. There are also two profiles (Top-Bottom and Bottom-Top). In both cases, the second sequence is conducted until failure (Fig. 3). Hereafter, they are denoted T-B and B-T.

Fig. 2 Two blocks multi-sequential loading schemes, a: (H-L), b: (L-H)

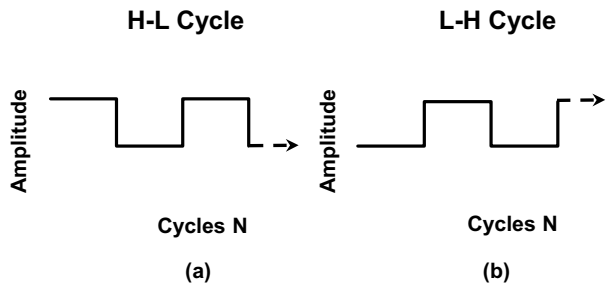
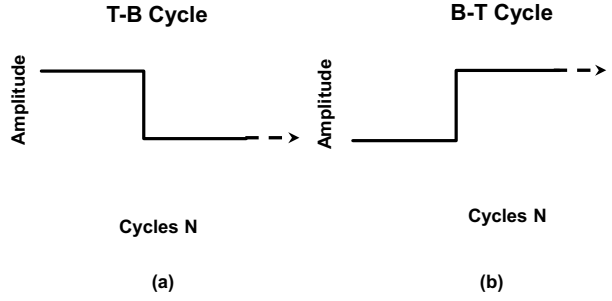


Fig. 3 Alternate Multi-block loading fatigue tests, **a:** (T-B), **b:** (B-T)



3 Hybrid Model and Multi-block Loading Fatigue Life Modeling

3.1 Hybrid Model

The micromechanical model [17] was originally proposed to predict S-N curves in the case of constant amplitude and temperature and variable microstructure. It was recently generalized in the case of variable temperature [20]. Moreover, the model can determine the evolution of the local damage rate, $\frac{d}{d_c}$ as a function of the stiffness reduction, $\frac{E}{E_0}$. The generated state equation is then given by the following equation:

$$\left(\frac{d}{d_c}\right) = \alpha \left[\left(\frac{E}{E_0}\right)\right]^2 + \beta \left[\left(\frac{E}{E_0}\right)\right] + \gamma \quad (1)$$

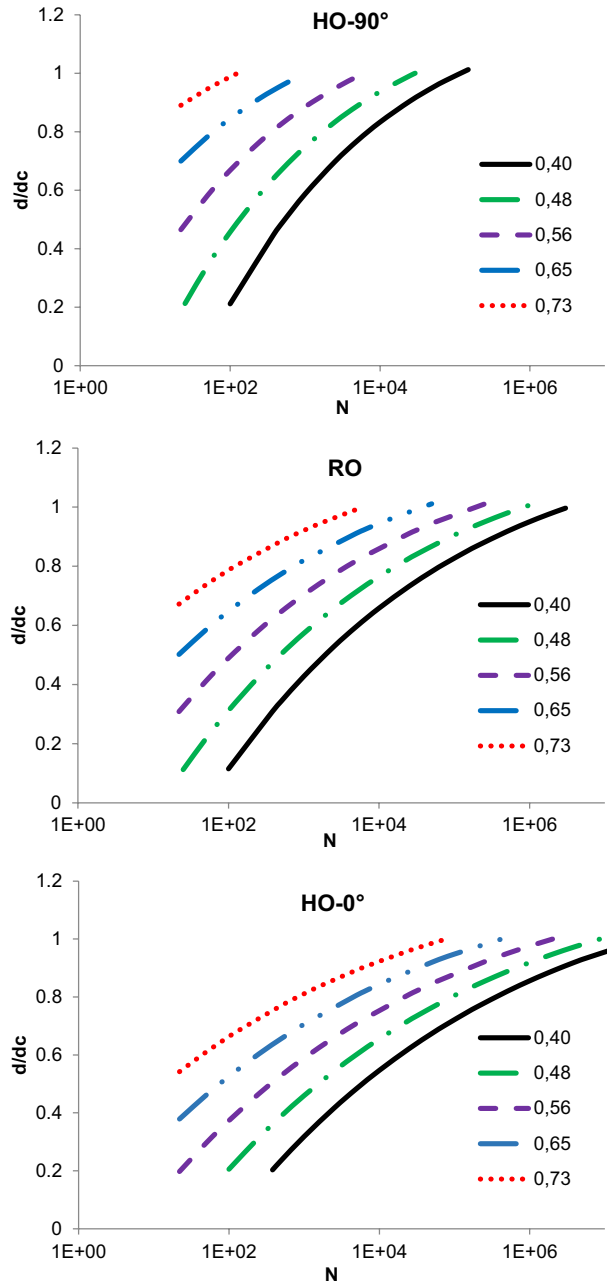
α , β and γ are micromechanical parameters identified on the basis of tensile modeling using reverse engineering (see [17] for more details). E_0 and E_D are Young's moduli of virgin and damaged material, respectively. This relation, identified in the case of monotonic tensile loading, is independent of the microstructure so that it could be considered as an equation of state relating microscopic damage state to macroscopic properties degradation. Therefore, this relationship is supposed to be accurate even for other loading schemes such as fatigue. The generalized expression giving the evolution of the local damage rate during fatigue as a function of macroscopic loss of stiffness is:

$$\left(\frac{d}{d_c}\right)_{(\sigma)} = \alpha \left[\left(1 + a(\sigma^{\text{imp}} - \sigma^S)\right) * \left[\frac{N}{N_S}\right]^B \right]^2 + \beta \left[\left(1 + a(\sigma^{\text{imp}} - \sigma^S)\right) * \left[\frac{N}{N_S}\right]^B \right] + \gamma \quad (2)$$

where σ^S and a are the threshold and kinetic of damage under monotonic tensile loading. These parameters are dependent on microstructure and can be identified experimentally or numerically using the micromechanical model. B is the kinetic of damage under fatigue determined experimentally (see [17] for more details). Therefore, the evolution of the local damage rate can be plotted as a function of the number of cycles for different macroscopic applied stresses (see Fig. 4). Note that in Fig. 4, the applied stress is normalized. Note also that this evolution may be plotted for other working temperatures: 80 and -30 °C useful in automotive applications. If so, the corresponding values of α , β , γ , a , σ^S and B should be identified in the same way.

Note that the resolution of Eq. 1 for $\frac{d}{d_c} = 1$ allows determining the expression of the number of cycles to failure versus the applied stress:

Fig. 4 Evolution of the local damage rate under fatigue loading for different microstructures and different normalized applied stress at 23 °C



$$N_R = N_S^* \left[\frac{G}{1 + a(\sigma^{\text{imp}} - \sigma^S)} \right]^{\frac{1}{\beta}} \quad \text{where } G = \frac{-\beta \pm \sqrt{\beta^2 - 4\alpha(\gamma - 1)}}{2\alpha} \quad (3)$$

Therefore predicted SN curve may be plotted and compared to the experimental ones for the different microstructures and loading direction. Good agreements in Fig. 5 confirm the efficiency of this approach. Note that in this figure HO-0° and HO-90° indicate highly oriented fibers for 0° (mold flow direction) and 90° tensile direction respectively. Moreover, in a recent paper [18], this predictive method has been validated for other working temperatures (-30 and 80 °C).

One can note that this methodology is proposed for the fatigue lifetime ranging between 10^3 and 10^5 cycles. This is appropriate based on the application of the SMC composite (automotive structures such as tailgates).

3.2 Variable Amplitude Fatigue Cumulative Damage Methodology

Cumulative damage state was computed in the case of the multi-block profiles defined in Fig. 2 (L-H and H-L) and 3 (T-B and B-T). For the validation, experimental multi-sequential L-H and H-L fatigue tests were performed on three specimens for each microstructure configuration (RO, HO-0° and HO-90°). Damage accumulation is computed stage after stage through the calculation of the evolution of the local damage ratio from Eq. 2 for every sequence $S_i = (\sigma_i, N_i)$. Indeed, Eq. 2 provides the evolution of the local damage rate for any mono-block configuration (σ_i, N_i) . In this approach, we suppose that the principle of superposition is verified. In other words, each sequence $S_i = (\sigma_i, N_i)$ follows the corresponding mono-block evolution described by Eq. 2. For each transition from one block to another, the number of cycles corresponding to the same local damage rate for the new value of the amplitude σ_{i+1} ,

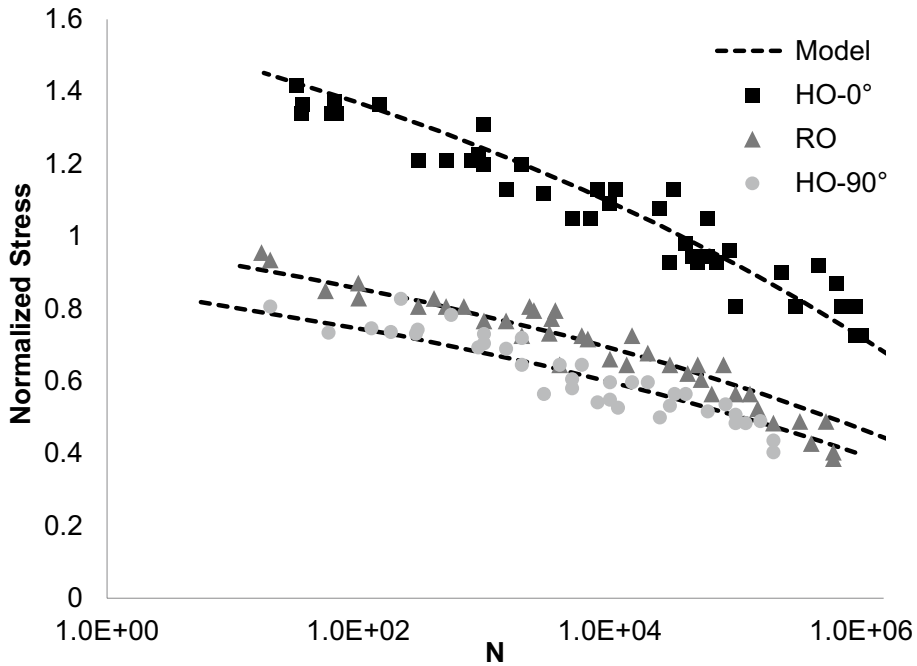


Fig. 5 Experimental and predicted Wöhler curves for different microstructure and test configurations at 23 °C

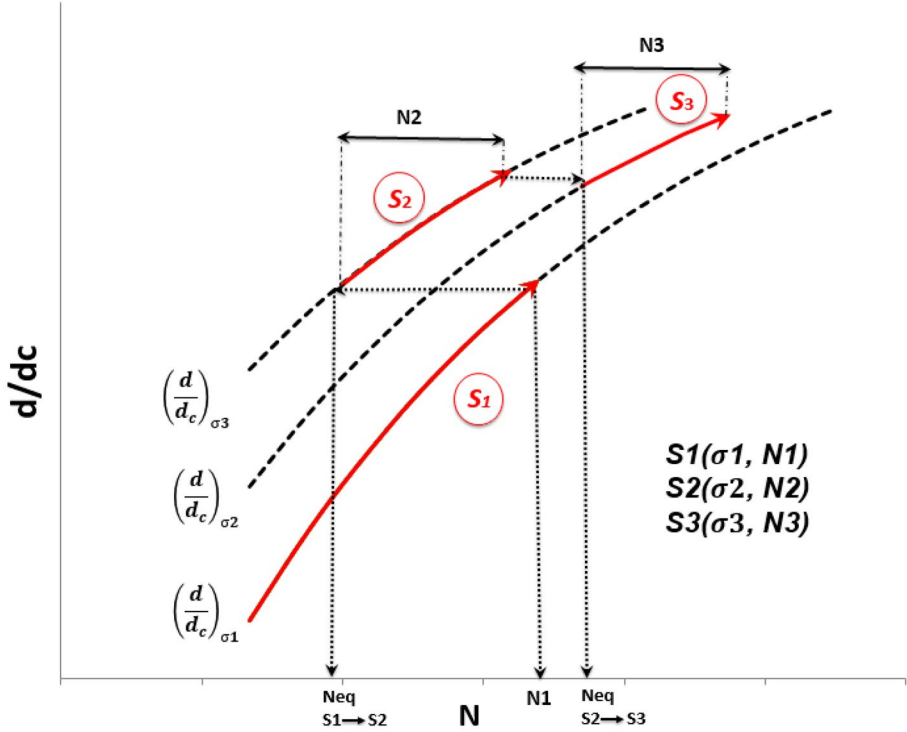


Fig. 6 Illustration of the cumulative damage methodology

N_{eq} , should be computed. Figure 6 illustrates graphically the determination of N_{eq} . One can see that to shift from the sequence "i" to the sequence "i + 1", the condition of the irreversibility of damage imposes that:

$$\left(\frac{d}{dc}\right)_{(\sigma_i, N_i)} = \left(\frac{d}{dc}\right)_{(\sigma_{i+1}, N_{eq})} \quad (4)$$

Therefore, the increment of local damage occurring during each new loading block is calculated using the corresponding new stress in Eq. 2 and considering an initial value determined for $N = N_{eq}$.

Therefore, once the micromechanical damage model is identified and validated, it can be used to predict the cumulative local damage until failure for a defined variable amplitude sequence.

Mathematically, one can determine the expression of N_{eq} applicable for each transition by introducing the condition of damage irreversibility into Eq. 2. This leads to:

$$N_{eq} = N_S^* \left[\frac{G}{((1 + a(\sigma^{imp} - \sigma^S))} \right]^{\frac{1}{\beta}} \quad (5)$$

$$\text{with } G = \frac{-\beta \pm \sqrt{\beta^2 - 4\alpha \left(\gamma - \left(\frac{d}{d_c} \right)_{(\sigma, N_i)} \right)}}{2\alpha}$$

Then, the value of the local damage rate at the end of the next sequence should be computed using Eq. 1 setting $\sigma = \sigma_{i+1}$ and $N = N_{i+1} + N_{eq}$. Finally, when $\frac{d}{d_c}$ exceeds 1 during a sequence S_i , the total number of cycles may be computed following the next equation :

$$N_R = N_S^* \left[\frac{G}{((1 + a(\sigma^{\text{imp}} - \sigma^S))} \right]^{\frac{1}{\beta}} - N_{eq} + \sum_{j=1}^{i-1} N_j \quad (6)$$

3.3 Variable Thermomechanical Multi-sequential Loading Algorithm

According to the above methodology, a predictive tool was developed based on the algorithm presented in Fig. 7. Note that the latter was developed for both variations of amplitude and temperature so that the predictive tool could allow computing any thermomechanical multi-sequential loading. Therefore, the micromechanical parameter α, β and γ , the threshold and kinetic damage parameters a, σ^S and B were identified using the same experimental and micromechanical methodology as for ambient temperature.

3.4 Results and Validation

An alternating amplitude fatigue experimental campaign including H-L and L-H sequences (Fig. 2) was carried out for the various microstructures. Three tests were carried out for each type of microstructure and type of sequence in order to demonstrate the reproducibility of the experimental results. Because of the high scattering microstructure well known in SMC composites, the microstructure of each specimen was firstly selected on the basis of ultrasonic measurements described in [19, 20].

Results obtained from the multi-block loading fatigue tests are summarized in Table 1. (Note that S indicates the specimen number). In this table are reported the predicted results using average kinetic and real kinetic. Indeed, one can use the average value of B identified from one-block fatigue test results or the real damage kinetics directly measured from the stiffness reduction slope during each fatigue block. In both cases, the prediction is in good agreement with the experimental result. Indeed, the percentage of prediction error ranges from about 3–15% if average kinetics are used while it ranges from about 6–14% if real kinetics are used. Globally, independently of the type of sequence (H-L or L-H), one can notice that failure is predicted from approximately 10% before the real failure. These results indicate that the developed model can be considered conservative. In view of the very good agreement between experimental and simulated results, one can conclude that the proposed approach is efficient for variable amplitude and load sequence effects predictions.

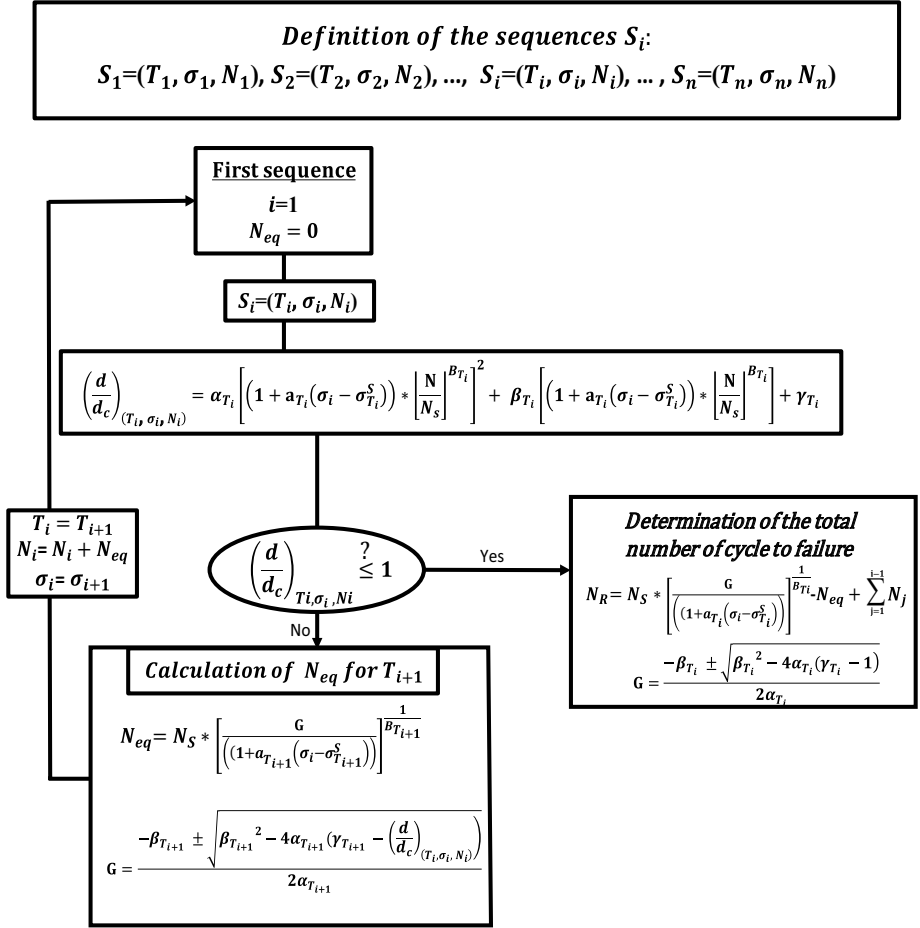


Fig. 7 Algorithm for multi-sequential thermomechanical loading including variable temperature and amplitude

4 Exploitation of the Model

Once the model is validated, it is interesting to use it in order to highlight the influence of different multi-blocks loading conditions.

4.1 Influence of the Order of Alternating Sequences

First, we propose to compare fatigue life obtained for High-Low sequence to that of Low-High sequence. In order to ensure that our analysis is not affected by the influence of the microstructure, we define two loading parameters as follows which will be fixed for all simulated configurations:

Table 1 Comparison and analysis between the experimental and the simulated results

		Prediction for different kinetics				Prediction error		
	Loading sequence (normalized stresses)	S	Cycle (sequence)	Nr	Average Kinetic	Real Kinetic	Average Kinetic	Real Kinetic
RO	H-L	1	20,000	69,300	50,000	64,000	-6,89%	-13,72%
	0.67-0.45 / 0.67-0.45	2	20,000	49,500		39,000		
		3	20,000	42,300		36,000		
	L-H	1	20,000	44,420	41,000	30,000	-3,39%	-11,25%
	0.45-0.67 / 0.45-0.67	2	20,000	39,200		35,000		
		3	20,000	43,700		48,000		
HO-0°	H-L	1	20,000	74,937	56,000	64,000	-11,87%	-17,12%
	0.95-0.65 / 0.95-0.65	2	20,000	62,200		45,000		
		3	20,000	53,500		49,000		
	L-H	1	20,000	72,030	50,000	68,000	-15,55%	-6,55%
	0.65-0.95 / 0.65-0.95	2	20,000	47,600		46,000		
		3	20,000	58,000		52,000		
HO-90°	H-L	1	20,000	74,050	60,000	64,000	-7,06%	-12,74%
	0.5-0.33 / 0.5-0.33	2	20,000	56,540		53,000		
		3	20,000	63,077		52,000		
	L-H	1	20,000	73,750	53,000	60,000	-6,70%	-11,33%
	0.33-0.5 / 0.33-0.5	2	20,000	45,060		51,000		
		3	20,000	51,600		40,100		

- $r = \frac{\sigma_H}{\sigma_L}$ which represents the ratio between the maximum stress σ_L reached during High loading and the minimum stress σ_L reached during Low loading. Thus, this parameter defines the amplitude variation between the two alternative blocks.
- $a = \frac{\sigma_H}{\sigma_r}$ which represents the ratio between the maximum stress σ_H and the failure stress σ_r under monotonous stress for the considered microstructure.

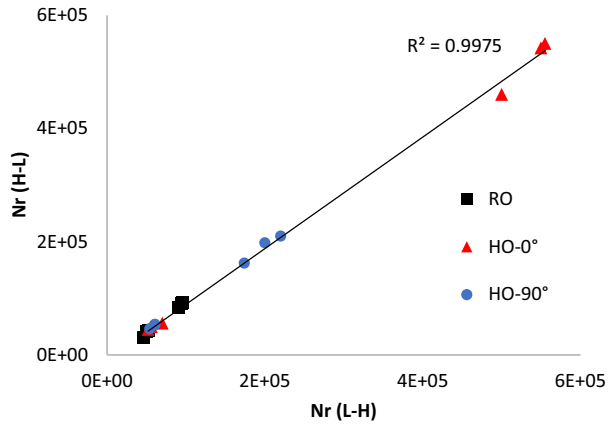
Three values of " a " and " r " were chosen (0.45-0.55-0.67) and (1.3-1.5-1.8) respectively. The fatigue life was computed for H-L and L-H sequences for each couple of parameters (a, r) and microstructure configuration: RO, HO-0° and HO-90°. The following table summarizes the results of this numerical study (Table 2).

One can see that H-L sequences fatigue life is still slightly higher than in the case of L-H sequences. However, Fig. 8, showing the predictions obtained in the case of Low-High sequences as a function of those High-Lows, highlights a slope close to 1. Consequently, we can conclude that in the case of alternating sequences, the order of the sequences has no real influence on the fatigue life whatever the microstructure considered.

Table 2 Summary of simulations carried out at variable amplitudes

	a	r	Average Kinetic prediction	
			H/L	L/H
RO	0.67	1.8	53,000	43,000
	0.67	1.5	50,000	41,000
	0.67	1.3	46,000	31,000
	0.55	1.8	96,000	92,000
	0.55	1.5	95,000	91,000
	0.55	1.3	90,000	84,000
	0.45	1.8	10 ⁷	10 ⁷
	0.45	1.5	10 ⁷	10 ⁷
	0.45	1.3	10 ⁷	10 ⁷
HO-0°	0.67	1.8	70,000	56,000
	0.67	1.5	56,000	50,000
	0.67	1.3	52,000	45,000
	0.55	1.8	555,000	550,000
	0.55	1.5	550,000	542,000
	0.55	1.3	500,000	460,000
	0.45	1.8	10 ⁷	10 ⁷
	0.45	1.5	10 ⁷	10 ⁷
	0.45	1.3	10 ⁷	10 ⁷
HO-90°	0.67	1.8	61,000	54,000
	0.67	1.5	60,000	53,000
	0.67	1.3	54,000	46,000
	0.55	1.8	220,000	210,000
	0.55	1.5	200,000	198,000
	0.55	1.3	174,000	162,000
	0.45	1.8	10 ⁷	10 ⁷
	0.45	1.5	10 ⁷	10 ⁷
	0.45	1.3	10 ⁷	10 ⁷

Fig. 8 L-H versus H-L sequences predictions



4.2 Two Blocks Variable Amplitude Loading (T-B, B-T)

In this part, we propose to study the effects of the loading with variable amplitude with two sequences such as defined in Fig. 3: T-B and B-T. The variability parameters that we propose to study are:

- The microstructure,
- The state of damage during the first cycle,
- The number of cycles during the first sequence,

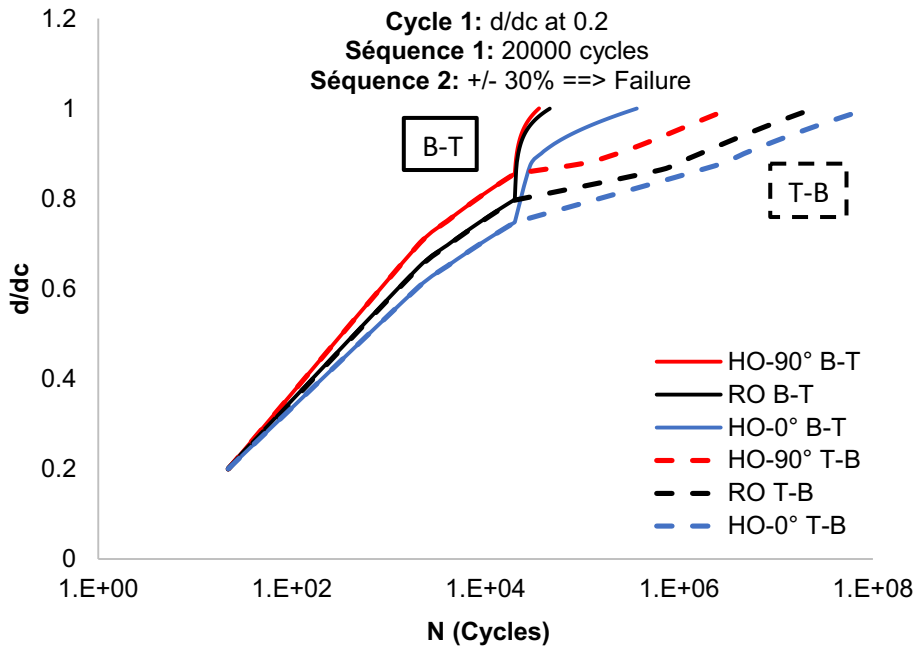


Fig. 9 Influence of the microstructure and the sequence order in the case of a variable loading with two sequences (T-B and B-T)

- The sequence order (T-B or B-T).

Figure 9 corresponds to the results obtained for loadings sequences such that during the first cycle a damage rate d/dc of 20% is reached. The amplitude of the first block is therefore chosen according to the corresponding microstructure. Then 20,000 cycles are applied with the same amplitude during the first loading block. Finally, a second loading block is applied until breaking with an amplitude 30% higher than the first block amplitude in the case of B-T loading and 30% lower in the case of T-B loading.

Figure 9 shows the obtained results. It clearly emphasizes the influence of the microstructure. Indeed, the damage kinetics obtained for the HO-90° microstructure are the most important and lead to premature rupture while those obtained for the HO-0° microstructure are slower and lead to later failure.

As expected, one notes that fatigue lives obtained in the case of T-B sequences are greater than those obtained in the case of B-T loading sequences. Indeed, in the second case, after a first sequence, there is an acceleration of the damage while in the first, the damage kinetics is lower due to reduced applied stress during the second block.

Subsequently, always with a chosen amplitude producing 20% damage in the first cycle, we varied the number of cycles in the first sequence from 10,000 to 30,000 cycles. Thus, the damage rates reached after the latter is variable. The curves of Fig. 10 show that the local damage rate reached at the end of the first sequence strongly influences the lifetime in the case of the B-T loading scheme whereas it has no influence in the case of T-B sequences. Note that this is verified independently of the microstructure.

Moreover, we studied the influence of the damage rate reached during the first cycle: from 20 to 40%. Figure 11 shows that it influences the lifetime of the two types of two blocks variable loading sequences (T-B and B-T). This is in line with the experimental

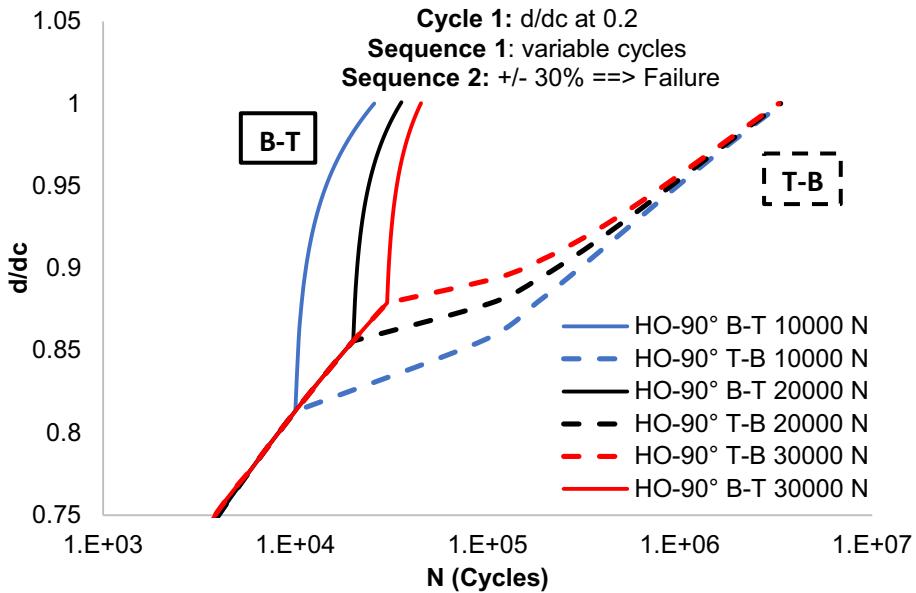


Fig. 10 Effect of the damage during the first sequence and the sequence order in the case of a variable loading with two sequences for an HO-90° material

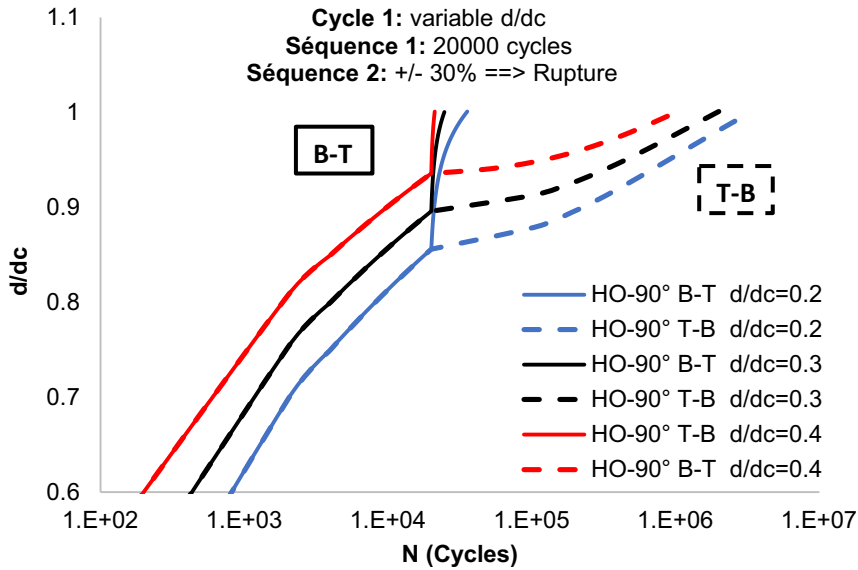


Fig. 11 Effect of the damage during the first cycle and the sequence order in the case of a variable loading with two sequences for an RO-90° material

observation discussed in previous papers [17, 21–29] relating the damage under monotonous loading and the fatigue life.

5 Conclusions

A hybrid model based on a phenomenological-micromechanical approach taking into account local fiber-matrix interfacial failure has been developed to calculate the evolution of the local damage in the case of an SFRC material submitted to several variable amplitude loading schemes. The model describes the accumulation of local damage from one sequence to another until a critical value. Indeed, the evolution of a unique local damage parameter is sufficient to predict any variable fatigue loading. Therefore, the equation of state generalized to fatigue loading can be used as a one variable phenomenological model in which the micromechanical parameters (α , β and γ) and the damage parameters (σ^S and a) should be identified for any microstructure using a simple monotonic tensile test simulation. The predictive efficiency of the approach has been demonstrated for three different SMC microstructures in the case of constant amplitude fatigue tests. Therefore, a general algorithm is proposed in order to predict the evolution of the local damage parameter (damage rate d/dc) in the case of variable amplitude loading sequences from constant amplitude damage predictions. Therefore, a cumulative damage prediction is performed as a function of the microstructure and the variable amplitude loading scheme. Finally, failure is assumed when the local cumulated damage rate reaches 1 ($d=dc$). Note that the proposed approach can be assumed as being a phenomenological residual local damage based model.

In order to validate the approach, an experimental campaign involving alternating low-high and high-low amplitude has been performed for three SMC microstructure

configurations. Predicted fatigue lives showed very good agreement with experimental findings. Once validated, the approach is used to highlight the effect of types and order of the cyclic sequences. Note that a recent paper [20], the efficiency of the proposed method has also been demonstrated in the case of variable temperature. Therefore, a general algorithm involving both variable amplitude and temperature is proposed.

Another significant highlight of our work is that the proposed model may be applied for any microstructure and three dimensional state of stress. Therefore, it could be used for real structure design involving the spatial distribution of microstructure. However, even if the efficiency of the proposed cumulative damage approach has been demonstrated in the case of the multi-block profile, it should be noticed that other fatigue parameters influences should be evaluated such as frequency and load ratio. Moreover, the presented approach should be improved in the case of thermoplastic composites for which the non-linear matrix behavior is interacting with damage at the local scale. Nevertheless, one can conclude that, although pragmatic and very simple to use, the proposed modeling has shown strong potential and a high level of relevance for SMC fatigue life prediction. In the near future, the model will be introduced into a finite element analysis and adapted for the fatigue design of SFRC structural components.

Data Availability All data generated or analysed during this study are included in this published article.

7. References

1. Fatemi, A.; L. Yang Cumulative fatigue damage and life prediction theories: a survey of the state of the art for homogeneous materials. *Int J Fatigue* **20**(1), 9–34 (1998)
2. Post, N.L., Case, S.W., Lesko, J.J.: “Modeling the variable amplitude fatigue of composite materials: A review and evaluation of the state of the art for spectrum loading”. Engineering Science and Mechanics, 106 Norris Hall, MC 219, Virginia Tech, Blacksburg, VA 24061, USA
3. Yang, L.; A. Fatemi Cumulative fatigue damage mechanisms and quantifying parameters: a literature review. *ASTM J Test Eval* **26**(2), 89–100 (1998)
4. Miner, M.A.: Cumulative damage in fatigue. *J. Appl. Mech* **12**, A159–A164 (1945)
5. Broutman, L., Sahu, S.: A new theory to predict cumulative fatigue damage in fiberglass reinforced plastics. In: Composite materials: testing and design (second conference) ASTM STP 497. 1972;170–88
6. Bond, I.P.: Fatigue life prediction for GR subjected to variable amplitude loading. *Composites Part A* **30**, 961–970 (1999)
7. Zago, A., Springer, G., Quaresimin, M.: Cumulative damage of short glass fiber reinforced thermoplastics. *J. Reinf. Plast. Compos.* **20**, 596–605 (2001)
8. Zago, A.; G. Springer Fatigue lives of short fiber reinforced thermoplastics parts. *J. Reinf. Plast. Compos.* **20**, 606–620 (2001)
9. Found, M.S., Quaresimin, M.: Two-stage fatigue loading of woven carbon fiber reinforced laminates. *Fatigue Fract Eng Mater Struct* **26**, 17–26 (2003)
10. Philippidis, T.P., Vassilopoulos, A.P.: Life prediction methodology for GFRP laminates under spectrum loading. *Composites Part A* **35**, 657–666 (2004)
11. Sonsino, C.; E. Moosbrugger Fatigue design of highly loaded short-glass-fibre reinforced polyamide parts in engine compartments. *Int J Fatigue* **30**, 1279–1288 (2008)
12. Dreißig, J., Jaschek, K., Büter, A., De Monte, M.: Fatigue life estimation for short fibre reinforced polyamide components under variable amplitude loading. In: 2nd International conference on material and component performance under variable amplitude loading. Darmstadt, Germany (2009)
13. Keiji Ogi, S., Yashiro, K., Niimi: A probabilistic approach for transverse crack evolution in a composite laminate under variable amplitude cyclic loading. *Compos. A* **41**, 383–390 (2010)
14. Hartmann, J., Moosbrugger, E.: A. BüterVariable amplitude loading with components made of short fiber reinforced polyamide 6.6. *Proc Eng* **10**, 2009–2015 (2011)

15. Eftekhari, M., Fatemi, A., Khosrovaneh, A.: Fatigue behavior of neat and short glass fiber reinforced polymers under two-step loadings and periodic over-loads, *SAE Int. J. Mater. Manuf.* (2016) 01e0373
16. Eftekhari, M., Fatemi, A.: Variable amplitude fatigue behavior of neat and short glass fiber reinforced thermoplastics. *Int. J. Fatigue* **98**, 176–186 (2017)
17. Laribi, M.A., Tamboura, S., Fitoussi, J., Tiébi, R., Tcharkhtchi, A.: H. Ben Dali. Fast fatigue life prediction of short fiber reinforced composites using a new hybrid damage approach: Application to SMC. *Composites Part B: Engineering*, Volume **139**, 155–162 (April 2018) 15
18. Jendli, Z., Meraghni, F., Fitoussi, J., Baptiste, D.: “Multi-scales modeling of dynamic behaviour for discontinuous fibre SMC composites” *Composites. Science and Technology* **69**, 97–103 (2009)
19. Tamboura, S., Sidhom, H., Baptiste, D.: “Evaluation de la tenue en fatigue du composite SMC R42”. *Matériaux et Techniques*, N° 3–4, p3.-11 (2001)
20. Tamboura, S., Laribi, M.A., Fitoussi, J., Shirinbayan, M., Tie Bi, R., Tcharkhtchi, A.: H. Ben Dali. Damage and fatigue life prediction of short fiber reinforced composites submitted to variable temperature loading: Application to Sheet Molding Compound composites. *Int. J. Fatigue* **138**, 105676 (2020)
21. Meftah, H., Tamboura, S., Fitoussi, J., Bendaly, H., Tcharkhtchi, A.: Characterization of a new fully recycled carbon fiber reinforced composite subjected to high strain rate tension. *Appl Compos Mater* **25**(3), 507–526 (2018)
22. Shirinbayan, M., Fitoussi, J., Abbasnezhad, N., Meraghni, F., Surowiec, B., Tcharkhtchi, A.: Mechanical characterization of a Low Density Sheet Molding Compound (LD-SMC): Multi-scale damage analysis and strain rate effect. *Compos Part B* 131 (2017)
23. Klimkeit, B., Nadot, Y., Castagnet, S., Nadot Martin, C., Dumas, C., Bergamo, S., et al: Multiaxial fatigue life assessment for reinforced polymers *Int J Fatigue* **33**, 766–780 (2011)
24. Bernasconi, A., Davoli, P., Basile, A., Filippi, A.: Effect of fibre orientation on the fatigue behaviour of a short glass fibre reinforced polyamide-6. *Int J Fatigue* **29**, 199–208 (2007)
25. De Monte, M., Moosbrugger, E.: M. Quaresimin Influence of temperature and thickness on the off-axis behaviour of short glass fibre reinforced polyamide 6.6 – cyclic loading. *Composites A Partie Appl Sci Manuf* **41**, 1368–13793 (2012)
26. De Monte, M., Moosbrugger, E., M. Quaresimin Influence of temperature and thickness on the off-axis behaviour of short glass fibre reinforced polyamide 6.6 – Quasi-static loading. *Composites Part A: Applied Science and Manufacturing*, Volume 41, Issue 7, July 2010, Pages 859 – 87
27. Arif, M.F., Saintier, N., Meraghni, F., Fitoussi, J., Chemisky, Y., G. Robert. Multiscale fatigue damage characterization in short glass fiber reinforced polyamide-66 *Compos B - Eng*, 61 (2014), pp. 55–65
28. Shirinbayan M*, Fitoussi, J., Meraghni, F., Surowiec, B., Laribi, M.A., Tcharkhtchi, A.: Coupled effect of loading frequency and amplitude on the fatigue behavior of advanced sheet molding compound (A-SMC). *J. Reinf. Plast. Compos.* **36**(4), 271–282 (2017)
29. Zuo, P., Benevides, R.C., Laribi, M.A., Fitoussi, J., Shirinbayan, M., Bakir, F., Tcharkhtchi, A.: Multi-scale analysis of the effect of loading conditions on monotonic and fatigue behavior of a glass fiber reinforced polyphenylene sulfide (PPS) composite. *Comp Part B: Engineering* **145**, 173–181 (2018)

Authors and Affiliations

M. A. Laribi^{1,2} · S. Tamboura³ · J. Fitoussi² · M. Shirinbayan^{2,4} · R. Tie Bi⁵ · A. Tcharkhtchi² · H. Ben Dali³

S. Tamboura
sahbi.tamboura@gmail.com

J. Fitoussi
joseph.fitoussi@ensam.eu

M. Shirinbayan
mohammadali.shirinbayan@ensam.eu

R. Tie Bi
bob.valor-ext@faurecia.com

A. Tcharkhtchi
abbas.tcharkhtchi@ensam.eu

H. Ben Dali
hachmi.bdaly@gmail.com

- ¹ Institut Clément Ader ICA, CNRS UMR 5312, 3, Rue Caroline Aigle, 31400 Toulouse, France
- ² CNAM, PIMM, Arts et Metiers Institute of Technology, HESAM University, F-75013 Paris, France
- ³ Ecole Nationale d'Ingénieurs de Sousse, LMS, Pôle technologique, 4054 Sousse, Tunisie
- ⁴ CNAM, LIFSE, Arts et Metiers Institute of Technology, HESAM University, F-75013 Paris, France
- ⁵ Zero Emission, FAURECIA CLEAN MOBILITY, 25550 Bois, Bavans, France